Advanced Physical Research
Vol.7, No.3, 2025, pp.292-303
https://doi.org/10.62476/apr.73292

MODELING OF WAVE PROCESSES IN A BROADBAND HORN ANTENNA FOR TRANSMITTING AND RECEIVING RADIO FREQUENCY MICROWAVE SIGNALS

I.J. Islamov[1*], R.G. Akhundov[2], Y. Iliev[3], D. Dimitrov[4], V. Panevski[4]

[1]Baku Engineering University, Baku, Azerbaijan
[2]National Defense University, Baku, Azerbaijan
[3]Nikola Vaptsarov Naval Academy, Varna, Bulgaria
[4]Institute of Metal Science, Equipment, and Technologies with Center for Hydro- and Aerodynamics "Acad. A. Balevski" at the Bulgarian Academy of Science, Sofia, Bulgaria

Abstract. In the article, the issue of modeling the 8-12 GHz frequency band horn antenna device used in radar and satellite radio communication systems was considered, its analysis and application areas were investigated. The investigated horn antenna operates in the microwave frequency range and has a simple construction that works effectively. Constructive models of the researched horn antenna in the H and E planes have been worked out, and mathematical modeling has been performed. Aluminum was used as the material of the antenna. S-parameter analysis was performed to evaluate the compatibility of the antenna with the feed line and energy losses. The frequency dependence of the reflection coefficient was established. 2D and 3D models of the directional diagram of the modeled horn antenna were constructed. The difference and advantages of the developed antenna from other antennas are shown. It was determined that the modeled horn antenna has a wide frequency range and at the same time has a simpler construction. Shown are the differences between the directional diagrams of the pyramidal antenna with a square opening in E- and H-planes. Mathematical models of horn antennas have been determined, such as the coefficient of antenna surface utilization, antenna directional diagrams with large phase errors, the width of the directional diagram at the half-power level, and ways to reduce the level of the side lobes of the antenna directional diagram have been identified. The gain of the loudspeaker antennas has been increased, the directivity has been improved, the operating frequency range has been increased, and the issues of good matching with waveguides have been resolved

Keywords: Modeling, wave processes, microwave signals, frequency, horn antenna, radar systems.
Corresponding author: I.J. Islamov, Baku Engineering University, Hasan Aliyev str., 120, AZ 0101, Baku, Azerbaijan, Tel.: +994 50 626 76 99, e-mail: *isislamov@beu.edu.az*
Received: 16 July 2025; Revised: 19 August 2025; Accepted: 25 August 2025; Published: 16 October 2025.

1 Introduction

Horn antennas belong to the class of aperture antennas, in which the directional radiation is formed and opened by a flat surface. The simplest aperture antenna is the open end of the waveguide. However, due to the relatively small size of the emitting aperture in relation to the wavelength, such an antenna has weak directivity. Horn antennas are used to increase directivity (Sharma et al., 2024; Dubrovka et.al., 2022; Bhardwaj et.al., 2018).

Horn antennas are one of the main types of antennas in the centimeter wave range. Simplicity of construction, convenience of performing calculations with a good match between theory and experiment, absence of losses in the power supply tract - these are the advantages that allow you to use this type of antenna for various practical purposes and use them as reference for conducting various measurements. The only disadvantage of the horn antenna is its long length. It is possible to reduce the length of the horn by placing a dielectric lens in it with an opening (aperture) that equalizes the phase distribution. The uniformity of the phase can be achieved both when using a homogeneous dielectric by changing its thickness and by using non-homogeneous media (Nishi et.al., 2024; Cho et.al., 2024).

Horn antennas are simple but effective types of antennas used to direct and propagate electromagnetic waves. Originally designed for use in radar systems, these antennas are now widely used in many fields such as telecommunications, space exploration, parabolic mirror antenna radiators, and military purposes. The widespread use of this antenna is due to its very easy production, easy feeding, practicality (convenience for use), and high gain Islamov et.al. (2022, 2023). The main function of horn antennas is to efficiently direct and propagate radio waves. These antennas perform particularly well in the extremely high frequency bands.

The X-band covers the frequency range of 8-12 GHz and has a wide range of uses in high-frequency communication and detection systems such as radar, satellite communications, air traffic control, and military applications (Zhang et. al., 2016, 2018). The wide frequency bandwidth and high resolution characteristics of this band make it essential for critical applications. The high frequency of the X-band makes it ideal for applications requiring high resolution and sensitivity, while allowing for antenna modeling in smaller sizes.

One of the main reasons for using horn antennas in the X-band is that these antennas provide low loss, high gain, and a wide frequency bandwidth (Tak et. al., 2017; Islamov et.al., 2023, 2022; Islamov , 2023). They also provide ease of manufacture and cost efficiency due to their simple structure. These features make horn antennas the preferred choice for applications requiring high performance in the X-band.

Horn antennas are widely used in microwave and millimeter wave frequencies due to their simple structure, high gain, and low loss (Zhang et. al., 2024; Zhao et. al., 2022). Their ability to efficiently direct the electromagnetic energy emitted from the waveguides into free space makes these antennas ideal for applications requiring high directivity and sensitivity. The most common types of horn antennas are the E-sector horn, H-sector horn, pyramidal, conical, and dual-ridged horn antennas:

- E-sector horn antennas are antennas created by expanding a waveguide in the E plane. They have a narrow frequency band and provide high gain at a given frequency. This antenna type is preferred in applications requiring high directivity and gain.

- H-sector horn antennas are a structure that creates radiation in the H-plane by expanding the parallel dimension of a traditional 3D horn antenna while keeping the perpendicular dimension constant (Luo et. al., 2023; Zoghi et. al., 2024; Yadav et. al., 2021). This antenna type provides high gain in a narrow frequency band, similar to the E-sector horn antennas.

- Pyramidal horn antennas are antennas that are expanded in both the E and H planes. This antenna type is the most widely used antenna type for X-band applications and is commonly used in radar and communication systems (Wang et. al., 2022). It has a wide frequency range and good directivity. It usually provides high gain, and for this, the aperture dimensions are usually large relative to the wavelength.

- Conical horn antennas are obtained by conically expanding a cylindrical waveguide and are preferred in applications requiring circular polarization (Jiangjun et. al., 2023; Islamov et.al., 2023; Islamov et. al., 2025). Wider cones provide higher gain and a narrow directivity pattern.

- Dual-ridged horn antennas are widely used in ultra-wideband applications (Islamov et. al., 2025). A characteristic feature of these antennas is the presence of two ridge structures placed inside the waveguide. These ridges provide a wide frequency range by reducing the impedance (resistance) of the antenna at low frequencies.

Horn antennas are one of the classic electromagnetic radiation devices, and find wide application in radio astronomy, satellite communications, radar, measurement devices, and especially in the millimeter (mmWave) and terahertz (THz) ranges. Among their advantages, high gain, good directivity, and compatibility with waveguides are particularly emphasized. However, against the background of the requirements of modern high-frequency communication systems, there are still open scientific and technological problems of horn antennas, which can be attributed to the following (Prabir et. al., 2025; Benjamin et. al., 2025; Kalyan et. al., 2024; **?**; Mahmoud et. al., 2025):

1. Application in high frequency ranges. Micron-level precision is required during the production of horn antennas operating in the terahertz range. Mechanical and technological errors can significantly change the radiation pattern of the antenna. Therefore, research is being conducted on new manufacturing methods based on 3D printing, micromachining and metamaterial technologies.

2. Size and mass reduction. Classic horn antennas are large in size, which is incompatible with miniaturization in modern devices. Dielectric horns, short-horn and hybrid structures are being developed to solve the problem. However, the optimal balance between efficiency and size has not yet been fully achieved.

3. Broadband and multiband operation. The demand for broadband antennas is increasing for 5G and future 6G systems. Traditional horns, on the other hand, operate efficiently mainly in narrow bands. Corrugated, log-periodic and variable-length horn types are proposed for this.

4. Polarization stability and multi-radiation. It is difficult to maintain polarization stability in loudspeaker antennas. Reducing sidelobes and eliminating multipath effects are current research topics.

5. Integration with phased arrays. Phased arrays play a key role in modern communication and radar systems. Integration of loudspeaker antennas with these arrays is complex, but research is underway on waveguide-loudspeaker hybrids in the THz range.

6. New materials and energy efficiency. At high frequencies, the losses of metals increase. For this reason, the development of loudspeaker antennas based on superconducting materials, graphene, and low-loss dielectrics is relevant. However, the application of such materials is currently mainly at the laboratory stage.

In the presented article, the gain of existing loudspeaker antennas has been increased, the directivity has been improved, the operating frequency range has been increased, and the issues of good matching with waveguides have been solved, which can also be considered a scientific innovation.

2 Modeling a horn antenna

The flare angle is a critical component of horn antennas and plays an important role in determining the directional pattern. A larger flare angle creates a wider directional pattern, since increasing the flare angle also increases the phase difference between the center and the edges. The values of the flare angles depend on the specific design and application of the antenna.

Choosing the appropriate flare angle allows you to optimize the directional pattern and gain. Figure 1 shows a cross-sectional view of a horn antenna. Figure 1, a, shows a cross-section along the H-plane, and Figure 1, b, shows a cross-section along the E-plane.

In the design of X-band horn antennas, the aperture width (a_1) and height (b_1) of the horn are determined by the wavelength (λ). To provide high gain, the aperture dimensions are usually chosen to be several times the wavelength. The flare angle (the angle at which the antenna's aperture opens) determines the angle at which the waves emerging from the waveguide propagate into free space and is usually chosen between 10 and 20 degrees Islamov et al. (2025).

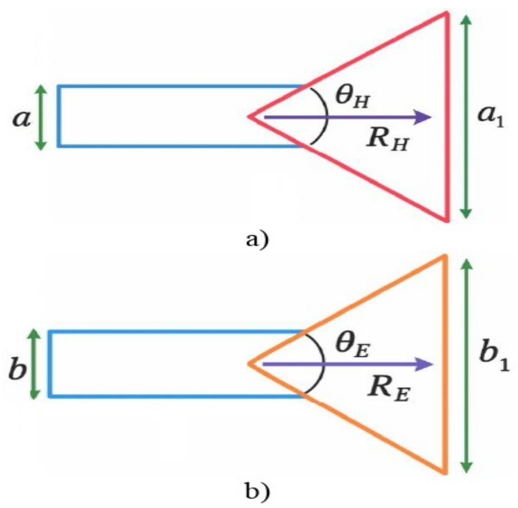

Figure 1: Cross-sectional view of the horn antenna: a- along the H-plane; b- along the E-plane

The width (a) and height (b) of the waveguide are selected taking into account the lower and upper frequency limits of the X-band. Impedance matching is achieved by optimizing the aperture angle and aperture dimensions. This matching is achieved between the input impedance and output impedance of the antenna using the conversion equations. The main design parameters that determine the performance of horn antennas are:

- Aperture size and shape: The aperture size of the horn antenna determines the antenna gain and the shape of the antenna beam pattern. Larger aperture sizes provide a narrower beam pattern and higher gain. The maximum aperture size of practical horns is limited to about 15 wavelengths.

- Horn length: The length of the horn affects the antenna beam pattern and bandwidth. Longer horns provide a narrower and more focused beam pattern. The length of the horn also affects the impedance matching of the antenna.

- Opening angles: The opening angles of a horn antenna affect the wave propagation and the antenna gain. Determining the optimal angles increases the antenna performance and ensures maximum efficiency in a given frequency range.

To design a pyramidal horn antenna, the desired gain G_0 and the dimensions a and b of the rectangular feed waveguide are usually known. The purpose of the design is to determine the remaining dimensions (a_1, b_1, ρ_e, ρ_h, P_e and P_h) that will provide optimal gain. These dimensions are the width of the horn opening a_1, the height of the horn opening b_1, the electrical dimension parameter ρ_e that determines the electric field performance of the horn, the magnetic dimension parameter ρ_h that determines the magnetic field performance of the horn, P_e and P_h, which are calculated from ρ_e and ρ_h and are related to the physical dimensions of the horn. The appearance of a pyramidal horn antenna is shown in Figure 2.

The opening values of the loudspeaker a_1 and b_1 are selected to ensure optimal directivity of the E- and H-plane sectorial loudspeakers, respectively, and are calculated using the following formulas (1), (2) (Sharma et al., 2024):

$$a_1 = \frac{G_0}{2\pi}\sqrt{\frac{3}{2\pi\chi}}\lambda, \tag{1}$$

$$b_1 = \sqrt{2\chi}\lambda, \tag{2}$$

where the parameter χ is used to calculate the gain factor and other design parameters of the horn antenna and is calculated by the following formula (3) Sharma et al. (2024):

$$\chi = \frac{G_0}{2\pi\sqrt{2\pi}}. \tag{3}$$

Horn antenna gain (G_0) is converted from dB to a dimensionless quantity in calculations. The amplification factor of the horn antenna is calculated by the formula (4) (Sharma et al., 2024):

$$\chi = \frac{G_0}{2\pi\sqrt{2\pi}}. \tag{4}$$

Electric and magnetic measurement parameters that determine the electric and magnetic field performance of the horn antenna are calculated by formulas (5), (6) (Sharma et al., 2024):

$$\frac{\rho_e}{\lambda} = \chi, \tag{5}$$

$$\frac{\rho_h}{\lambda} = \frac{G_0^2}{8\pi^3}\left(\frac{1}{\chi}\right). \tag{6}$$

In a pyramidal horn antenna, P_e and P_h must be equal and are defined as follows:

$$P_e = (b_1 - b)\left[\left(\frac{\rho_e}{b_1}\right)^2 - \frac{1}{4}\right]^{\frac{1}{2}}, \tag{7}$$

$$P_h = (a_1 - a)\left[\left(\frac{\rho_h}{a_1}\right)^2 - \frac{1}{4}\right]^{\frac{1}{2}}, \tag{8}$$

For a rectangular horn, the directional diagram is calculated using the equation:

$$D(\theta,\varphi) = \sin c^2\left(\frac{ka}{2}\sin\theta\cos\varphi\right)\cdot \sin c^2\left(\frac{kb}{2}\sin\theta\sin\varphi\right), \tag{9}$$

where $k = \frac{2\pi}{\lambda}$ is the wavenumber, a and b are the dimensions of the opening along the axes, and λ is the length of the wave.

After calculating the dimensions of the antenna, the most suitable dimensions were determined by optimizing them using CST Microwave Studio. In CST Microwave Studio, the mesh parameters, boundary conditions, and solver parameters are customized for each specific simulation. Automatic meshing, adaptive to the model geometry, is standard. Boundary conditions are selected based on the type of structure and frequency being modeled, and solver parameters are customized to achieve the required accuracy and computational efficiency. CST Microwave Studio automatically generates a mesh adapted to the model geometry.

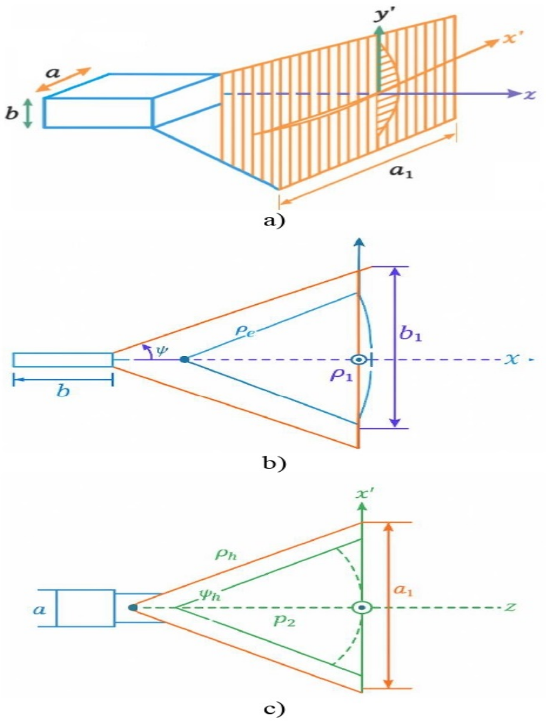

Figure 2: Pyramidal horn antenna: a- pyramidal horn; b- E-plane image; c- H-plane image

This simplifies the modeling process and allows you to focus on the design. The mesh is automatically refined in areas where it is needed to improve accuracy. This allows you to optimize the number of grid cells and reduce the calculation time. Increasing the mesh size can improve accuracy, but increases the calculation time. Choosing the optimal mesh size requires a trade-off between accuracy and calculation time. They are used to model conductive surfaces. CST Microwave Studio provides different types of solvers, such as finite element method (FEM) or finite difference time domain (FDTD) solvers. In FDTD solvers, the time step determines the discretization in time. It must be small enough to ensure the stability of the calculation. All dimensions of the modeled antenna are given in Table 1.

Table 1: Parameters of the Modeled Horn Antenna

Parameter	Dimensions, mm
Opening price of the speaker (a_1)	67
Opening price of the speaker (b_1)	45
Length of the speaker (L)	86
Length of the waveguide	20

3 Results and discussion

In this section, critical parameters such as gain, directivity, VSWR (Standing Wave Ratio), directivity pattern, and reflection coefficient are investigated to evaluate the performance of a loudspeaker antenna operating in the X-band. The results obtained for these parameters are explained in detail. According to the modeling parameters, the loudspeaker antenna is modeled in CST MWS. Figure 3 shows the modeled horn antenna.

For simulation purposes, the frequency ranges from 7 GHz to 13 GHz were selected. Aluminum was used as the antenna material. Aluminum horn antennas have a number of characteristics, including a wide frequency range, high gain, low standing wave ratio (VSWR), and the ability to operate in various climatic conditions. Aluminum provides strength and lightness of construction, as well as good electrical conductivity for efficient operation of the antenna. Aluminum is a good conductor of electricity. Its specific electrical resistance is 0,028 Ohm mm^2m. Aluminum has high electrical conductivity (37x10^6 S/m). S-parameter analysis was performed to evaluate the antenna's feedline compatibility and power losses. The reflection coefficient curve is shown in Figure 4.

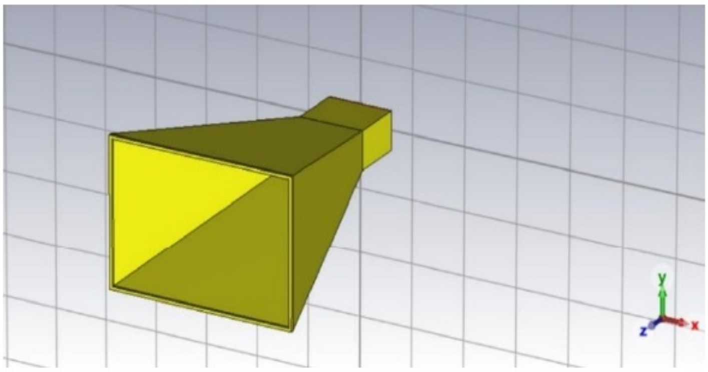

Figure 3: Modeled horn antenna

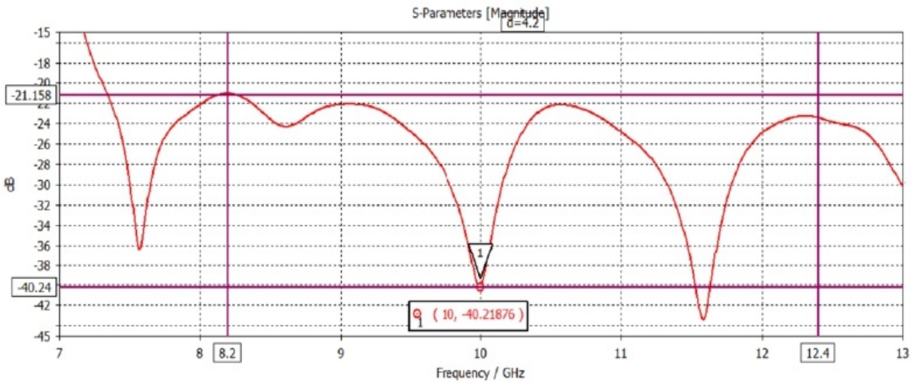

Figure 4: Reflection coefficient curve for a modeled horn antenna

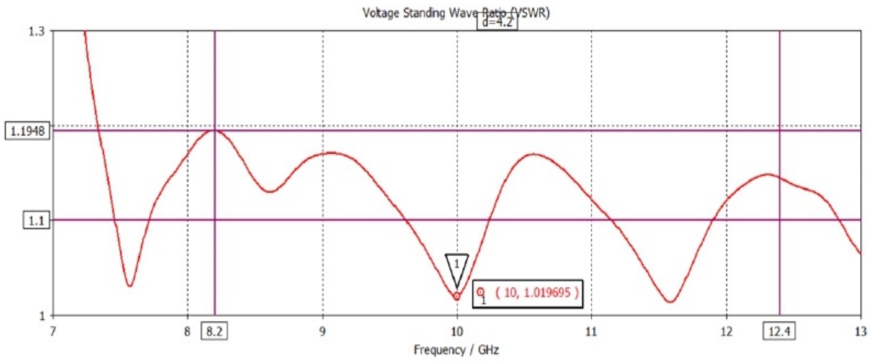

Figure 5: VSWR dependence of the modeled horn antenna

The VSWR graph showing the correspondence between the input impedance of the antenna and the resistance of the feed line is shown in Figure 5. A low VSWR indicates that the antenna provides maximum power transfer and that reflections are minimized. As can be seen, a low VSWR is achieved in the X band.

The obtained directivity is shown in Figure 6. The directivity indicates the performance of the antenna in certain directions. The directivity was found to be 15,5 *dB*.

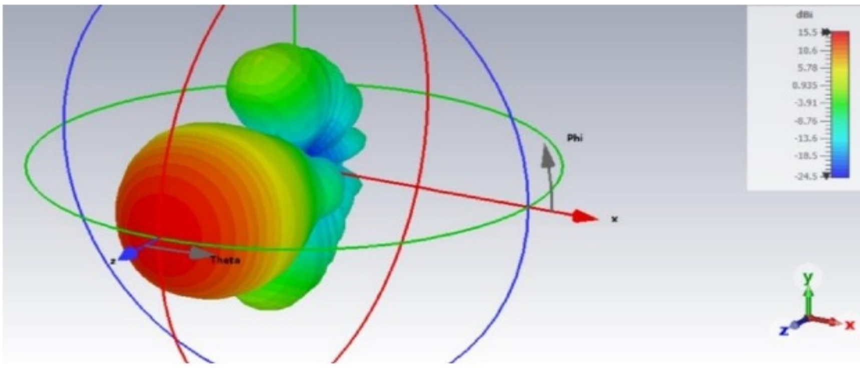

Figure 6: 3D directivity diagram model for the directivity coefficient of a modeled horn antenna: rad. effic. = -0,03593 *dB*, tot. effic. = -0,03635 *dB*, rizd. gain = 15,44 *dBi*

The obtained gain coefficient is shown in Figure 7. The gain coefficient is the ratio of the electromagnetic energy radiated by the antenna in a given direction to the energy radiated by an ideal isotropic antenna, and a high gain coefficient indicates the ability of the antenna to transmit electromagnetic waves over longer distances. The gain coefficient of the modeled horn antenna was found to be 15,4 *dB*.

A 2D directivity diagram is shown in Figure 8 and Figure 9. A directivity diagram is a graphical representation of the electromagnetic energy radiated by an antenna in different directions.

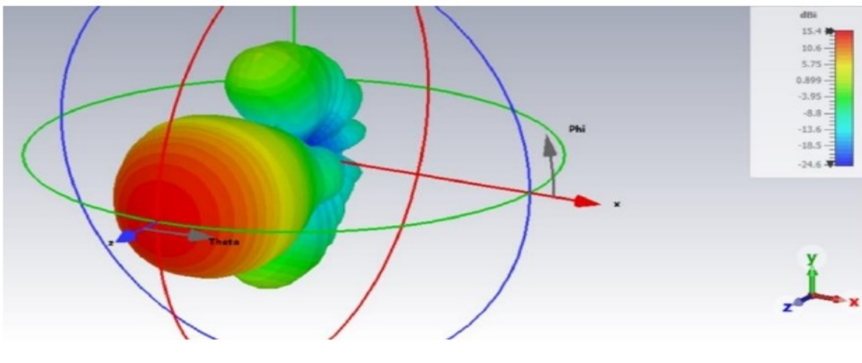

Figure 7: 3D directivity diagram model showing the gain of the modeled horn antenna: rad. effic. = -0,03593 *dB*, tot. effic. = -0,03635 *dB*, rizd. gain = 15,44 *dBi*

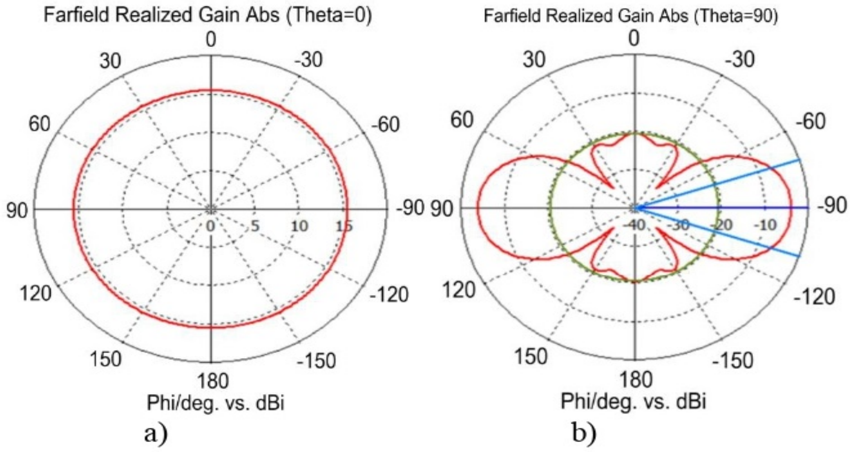

Figure 8: Directional diagram of a horn antenna: a- when $\theta = 0°$, main lobe magnitude=15,4 *dBi*; b- when $\theta = 90°$, main lobe magnitude=-4,04 *dBi*, main lobe direction=-90 deg., angular width (3 *dB*)=36,8 deg., side lobe level=-16,5 *dB*

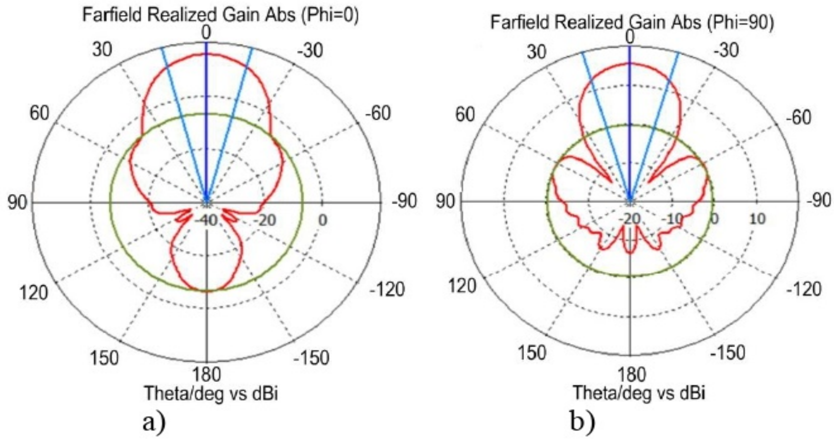

Figure 9: Polar plot of the ground angle of the modeled horn antenna: a- when $\theta = 0°$, main lobe magnitude=15,4 *dBi*, main lobe direction=0,0 deg., angular width (3 *dB*)=29,9 deg., side lobe level=-22,1 *dB*; b- when $\theta = 90°$, main lobe magnitude=-4,04 *dBi*, main lobe direction=-90 deg., angular width (3 *dB*)=36,8 deg., side lobe level=-16,5 *dB*

Horn antennas operating in the X-band typically provide high gain and directivity, making them ideal for radar and satellite communications applications. A summary of the simulated results is given in Table 2. Comparison of the simulation results with existing works is shown in Table 3.

Table 2: Simulation Results of the Modeled Antenna

Parameter	Dimensions	Unit
Bandwidth	8,2-12,4	*GHz*
Directionality	15,5	*dB*
Amplification	15,4	*dB*
Reflection coefficient in bandwidth	-22	*dB*
Reflection coefficient at 10 *GHz*	-40	*dB*
VSWR	1,2	-

Table 3: Comparison of simulation results with existing works

References	Employed frequen-cy, *GHz*	Direc-tivity coef-ficient, *dB*	Amplifi-cation factor, *dB*	The reflection coefficient at the first reso-nant frequency, *dB*	VSWR at the first resonant frequency
Prabir et al. (2025)	2-12	11,8	13,11	-36,1912	1,33
Benjamin et al. (2025)	2,1-12	11,7	12,65	-34,7649	1,27
Kalyan et al. (2024)	2,4-12	11,9	10,97	-37,4571	1,35
Hai-Xu et al. (2025)	1,5-12	11,9	11,76	-35,3421	1,37
Mahmoud et al. (2025)	1,7-12	12,1	12,57	-22,0836	1,39
This work	1,4-12,4	15,5	15,4	-26,7111	1,2

4 Conclusion

In this article, the modeling principles, performance analysis, and simulation studies of loudspeaker antennas operating in the X-band (8-12 *GHz*) have been investigated in detail. The results obtained show that loudspeaker antennas provide ideal solutions for high-frequency applications in the X-band. The modeled loudspeaker antenna showed high performance (efficiency) by providing 15,4 *dB* of gain. The directivity of the antenna was found to be 15,5 *dB*, which ensured high performance in certain directions. The match between the input impedance of the antenna and the resistance of the feed line was successfully achieved and low VSWR values were achieved. The VSWR was measured to be 1,2 in the 8,2-12,4 *GHz* bandwidth, which provides maximum power transfer and low losses. The reflection coefficient at 10 *GHz* was obtained to be -40 *dB*, which increases the efficiency of the antenna. The antenna provided a wide frequency range in the 8,2-12,4 *GHz* frequency range. The narrow main lobe and small side lobe levels ensure that the antenna performs well in certain directions. The information obtained was used to optimize the antenna performance and necessary improvements were made. X-band horn antennas provide reliable and efficient solutions for applications requiring high performance. With the development of technology, X-band horn antennas will continue to be a critical component in future communication and detection systems.

Acknowledgement
This publication was carried out under project G7475, funded by the NATO Science for Peace and Security Programmed.

References

Bhardwaj, S., Volakis, J.L. (2018). Hexagonal waveguide based circularly polarized horn antennas for sub-mm-wave/terahertz band. *IEEE Trans. Antennas Propag., 66*(7), 3366-3374.

Benjamin, S.C., Dejan, S.F. (2025). A Method for Reducing High-Frequency Sidelobes of a Millimeter-Wave Double-Ridged Horn Antenna. *IEEE Transactions on Antennas and Propagation*, *73*(6), 4098-4103.

Dubrovka, R., Andy, A.S., Saleh, E., Jones, R.C., Donnan, R.S., & Tuck, C.J. (2022). Additive manufacturing of a terahertz back-to-back horn antenna for use in life sciences. *IEEE Trans. Compon. Packag. Manuf. Technol., 12*(4), 595-601.

Cho J.-H., Park K.-Y., Lim C.-M., & Son H.-W. (2024). Design and Implementation of an X-Band Horn Antenna With a Metamaterial Lens Using 3D Printing Technology. *IEEE Access*, 12, 17773-17781.

Hai-Xu, L., Yong-Hong, Z., & Xiao-Dong, G. (2025). A Broadband High-Power Mode Transducer Used for Horn Antennas. *IEEE Antennas and Wireless Propagation Letters,* 24(5), 1233-1237.

Kalyan, M.P., Gowrish, B., & Hjalti, S. (2024). An Innovative Design Methodology of a Novel Multifunctional All-Pole Filtering Horn Antenna. *IEEE Microwave and Wireless Technology Letters, 35*(1), 35-38.

Islamov, I.J., Hunbataliyev, E.Z., & Zulfugarli, A.E. (2022). Numerical Simulation of Characteristics of Propagation of Symmetric Waves in Microwave Circular Shielded Waveguide with a Radially Inhomogeneous Dielectric Filling. *Journal of Microwave and Wireless Technologies, 14*(6), 761-767.

Islamov, I., Bashirov, R., & Ismayilov, N. (2023). Modeling of a Telecommunication Optical Waveguide with Anisotropic Medium. *International Journal of Microwave and Optical Technology, 18*(5), 131-139.

Islamov, I., Safarli, A. (2023). Design, Modelling and Research of an Antenna System for Transmitting and Receiving Information in Satellite Systems. *Transport and Telecommunication, 24*(3), 297-308.

Islamov, I., Humbataliyev, E. (2022). General Approaches to Solving Problems of Analysis and Synthesis of Directional Properties of Antenna Arrays. *Advanced Electromagnetics*, *11*(4), 22-33.

Islamov, I. (2023). Optimization of Broadband Microstrip Antenna Device for 5G Wireless Communication Systems. *Transport and Telecommunication*, *24*(4), 409-422.

Islamov, I.J., Aslanzadeh, I.A. (2023). Simulation of the Electromagnetic Field of a Microwave Waveguide Taking into Account the Anisotropy of the Medium. *Advanced Physical Research*, *5*(3), 168-176.

Islamov, I.J., Agayev, F.G., & Aliyeva, G.V. (2025). Electrodynamic Modeling of a Planar Antenna System for Wireless Communication. *Advanced Physical Research, 7*(1), 87-101.

Islamov, I.J., Akhundov, R.G., Dimitrov, D., & Panevski, V. (2025). Modeling of a Circular Disk Monopole Antenna Fed from a Microwave Broadband Coplanar Waveguide. *Advanced Physical Research, 7*(2), 184-195.

Jiangjun, Y., Jianying, L., Shigang, Z., Dong, L., & Guangwei, Y. (2023). A Polarization and Frequency Reconfigurable Microstrip Antenna for Vehicular Communication System Application. *IEEE Transactions on Vehicular Technology, 72*(1), 623-631.

Luo, Y., Zhao, S., Yan, N., An, W., Ma, K., & Meng, F. (2023). A Multicompressed-High-Order Modes Dipole Antenna With Wide-Beam and High-Gain Radiations in Two Different Bands. *IEEE Antennas and Wireless Propag. Lett., 22*(6), 1231-1235.

Mahmoud, G., Shoukry, I.S., Mahmoud, E., & Ghyslain, G. (2025). Design of Corrugated Horn Antenna for LEO Satellite Feeding System: Efficient Hybrid Optimization Approach. *IEEE Access,* 13, 92730-92739.

Nakprasit, K., Sakonkanapong, A., & Phongcharoenpanich, C. (2020). Elliptical ring antenna excited by circular disc monopole for UWB communications. *International Journal of Antennas and Propagation,* 8707182, 176-186.

Nishi, S., Tamesue, K., Sato, T., Myint, S.H., Sato, T., & Kawanishi, T. (2024). Design and Evaluation of a Lens Horn Antenna in the 300 GHz Band. *International Workshop on Antenna Technology,* 456-468.

Prabir, G., Zhao-Hong T., Sheng-Chun, T., Chih-Han, L., & Yu-Hsiang, C. (2025). A Semi-Open Substrate Integrated Horn Antenna with Dielectric Loading in 300 GHz Band. *IEEE Transactions on Terahertz Science and Technology*, 1-7.

Sharma, A., Kumar, D.V. (2024). Investigation of a Superstrate Loaded Ultrawideband Dual-Ridged Terahertz Pyramidal Horn Antenna. *IEEE Antennas and Wireless Propagation Letters*, *23*(12), 4533-4537.

Tak, J., Kang, D., & Choi, J. (2017). A lightweight waveguide horn antenna made via 3D printing and conductive spray coating. *Microw. Opt. Technol. Lett., 59*(3), 727-729.

Wang, Y., Li, T., & Dou, W. (2022). Ultrawideband 3-D printed endfire TEM horn antenna mounted on a cylinder conductor. *IEEE Antennas Wireless Propag. Lett., 22*, 2022-2026.

Yadav, S.V., Chittora, A. (2021). A compact ultra-wideband transverse electromagnetic mode horn antenna for high power microwave applications. *Microw. Opt. Technol. Lett., 63*(1), 264-270.

Zhang, B., Zhan, Z., Cao, Y., Gulan, H., Linnér, P., & Sun J. (2016). Metallic 3-D printed antennas for millimeter- and submillimeter wave applications. *IEEE Trans. THz Sci. Technol., 6*(4), 592-600.

Zhang, B., Li, R., Wu, L., Sun, H., & Guo, Y.-X. (2018). A highly integrated 3-D printed metallic K-band passive front end as the unit cell in a large array for satellite communication. *IEEE Antennas Wireless Propag. Lett.*, *17*(11), 2046-2050.

Zoghi, M., Hodjatkashani, F., & Lajevardi, M.E. (2024). A Low Distortion Radiation Pattern Ultra-Wideband TEM Horn Antenna. *IEEE Open Journal of Antennas and Propagation*, *5*(6), 1671-1680.

Zhang, B., Du, W., Liu, N., & Fu, G. (2024). Dielectric-Loaded Horn Antenna Design and Simulation Using the Metamaterial Method. *Electronics*, *13*(6), 1089.

Zhao, W., Li, X., Qi, Z., & Zhu, H. (2022). Broadband and High-Gain High-Order-Mode Fed Open-Ended Waveguide Antenna Array for Millimeter-Wave Applications. *IEEE Trans. Antennas Propag., 70*(9), 8614-8619.